# Supporting Information

## Ru Incorporated into Se Vacancy-containing $CoSe_2$ as Efficient Electrocatalysts for Alkaline Hydrogen Evolution

Li Liu[a,b], Ziyi Yang[a,b], Weibo Gao[c], Jianghuan Shi[c], Jieyun Ma[d], Zongjian Liu[a]*, Lin Wang[b,e]*, Yichao Wang[f]* and Zhengfei Chen[b]*

[a]College of Chemical Engineering, Zhejiang University of Technology, Hangzhou, Zhejiang 310014, China.

[b]School of Biological and Chemical Engineering, Ningbo Tech University, Ningbo, Zhejiang 315100, China.

[c]Ningbo Institute of Measurement and Testing (Ningbo Inspection and Testing Center for New Materials), Ningbo, Zhejiang 315048, P. R. China.

[d]School of Nursing and Midwifery, Faculty of Health, La Trobe University, Bundoora, Victoria 3083, Australia

[e]College of Engineering, Northeast Agricultural University, Harbin 150030, China

[f]School of Science, RMIT University, Melbourne, VIC 3000, Australia

Corresponding authors: zjliu@zjut.edu.cn (Z. Liu); l.wang@nit.zju.edu.cn (L. Wang); yichao.wang@rmit.edu.au (Y. Wang); zhengfei.chen@nit.zju.edu.cn (Z. Chen)

## Experimental section

### Characterization method

The morphology of all prepared materials was examined using a field emission scanning electron microscope (FESEM, Hitachi SU-8010). The elemental composition was further analyzed by an energy dispersive X-ray spectroscopy (EDX) analyzer (Oxford X-max80). High resolution transmission electron microscopy (HRTEM) and transmission electron microscopy (TEM) results were characterized on a JEM-2100. Powder X-ray diffraction (XRD) tests were analyzed at X-pert Powder, PANalytical B.V. The results were analyzed using a Thermo Fisher Scientific Escalabrator. X-ray photoelectron spectroscopy (XPS) tests were performed using Thermo Fisher Scientific Escalab 250Xi and AI Kα radiation.

### Electrochemical Measurements

All electrochemical measurements were carried out on an electrochemical workstation (CHI 760E) in 1.0 M KOH electrolyte, with Hg/HgO and graphite rods used as reference and counter electrodes, respectively. A glassy carbon electrode (GCE, 3 mm diameter) with loaded catalyst was used as the working electrode. Typically, the catalyst ink was prepared by dispersing 10 mg of sample in a mixture of ethanol (900 μL) and 1.0 wt.% Nafion solution (100 μL), followed by sonication. 4 μL of ink was loaded onto the GCE to achieve a loading of 0.57 $mg \cdot cm^{-2}$ and dried at ambient temperature. All potentials were converted to reversible hydrogen electrodes (RHE) via the Nernst equation:

$$E_{RHE} = \mathrm{E}_{Hg/HgO} + 0.0591 \times pH + 0.098 \quad (1)$$

First, the working electrode was stabilized using cyclic voltammetry (CV) and scanned until the curves almost overlapped. To obtain the polarization curves, linear scanning voltammetry with a scan rate of 5 $mV \cdot s^{-1}$ was performed. All polarization curves were calibrated by iR correction. Electrochemical stability was tested by performing 2000 CV cycles. Durability tests were performed using the chrono current method. Electrochemical impedance spectroscopy

(EIS) was performed over a range of 100 K to 0.01 Hz with an AC amplitude of 10 mV. Cyclic voltammetry (CV) measurements were performed at different scan rates to estimate the electrochemical double layer capacitance ($C_{dl}$) of the different electrocatalysts, and then the electrochemically active surface area (ECSA) was evaluated based on a proportional relationship.

**Tafel plots:** The Tafel plots are obtained from the corresponding LSV curves according to the Tafel equation $\eta = a + b \log j$ ($\eta$ is the applied overpotential, a is the Tafel constant, b is the Tafel slope, and j is the current density).

**Electrochemically active surface area (ECSA) calculation:** The electrochemically active surface area (ECSA) of the catalysts was estimated from the electrochemical double-layer capacitance ($C_{dl}$, mF), which was measured by cyclic voltammetry (CV) in 1.0 M KOH solution at scan rates ranging from 20 to 120 $mV \cdot s^{-1}$ at voltages of 0.05 to 0.15 V (with respect to the RHE) and the $C_{dl}$ value was derived from the equation:

$$C_{dl} = \frac{\Delta J}{2v} \quad (2)$$

where ν is the scan rate and ΔJ is the current difference at 0.1 V (relative to RHE).

The ECSA can be calculated using the following equation:

$$ECSA = \frac{C_{dl}}{C_s} \quad (3)$$

The specific capacitance is typically in the range of 0.02-0.06 mF $cm^{-2}$ and is assumed to be 0.04 mF $cm^{-2}$ in the ECSA calculation. The calculated ECSA value for Ru-$V_{Se}$-$CoSe_2$ was 81.9 $cm^{-2}_{ECSA}$, while the ECSA values for the Ru-$CoSe_2$, $V_{Se}$-$CoSe_2$ and $CoSe_2$ were 56.9, 24.3, and 16.3 $cm^{-2}_{ECSA}$, suggesting more exposed active sites of Ru-$V_{Se}$-$CoSe_2$.

**Activation energy calculation:** The polarization curves of the Ru-$V_{Se}$-$CoSe_2$ catalyst were tested at different temperatures before calculating log $j_0$ through the Tafel slope and then the

electrochemical activation energy according to the Arrhenius equation:

$$\log j_0 = \log(\mathrm{F}K_C) - \frac{\Delta G_0}{2.303RT} \quad (5)$$

where R is the gas constant, $\Delta G_0$ is the apparent activation energy, F is the Faraday constant, and $K_c$ is the equilibrium constant.

**Kinetic isotope effects:** The electrocatalysts were subjected to polarization curves in 1.0 M KOH aqueous solution and 1.0 M KOH $D_2O$ solution, respectively, and the current densities at a certain overpotential η were abbreviated as $j_{H2O}$ and $j_{D2O}$, and then the equation for the KIEs (H/D) was as follows:

$$KIEs_{H/D} = \left[\frac{K_{H2O}}{K_{D2O}}\right]_\eta = \left[\frac{j_{H2O}}{j_{D2O}}\right]_\eta \quad (6)$$

where the current densities of $j_{H2O}$ and $j_{D2O}$ were compared at a potential of -0.19 to -0.24 V (vs. RHE).

**Mass activity calculations**: In order to compare the mass activities of Pt/C, Ru-$V_{Se}$-$CoSe_2$ and Ru-$CoSe_2$, their activity values have been normalized to the Pt/Ru loading. An overpotential of -0.2 V was chosen to evaluate the mass activity. The specific equations are as follows:

$$j_{mass}^{Ru-V_{Se}-CoSe_2} = \frac{j_{area}^{Ru-V_{Se}-CoSe_2}(mA\ cm^{-2})}{mass_{Ru}} = 44.1\ A{\cdot}mg^{-1} \quad (7)$$

$$j_{mass}^{Ru-CoSe_2} = \frac{j_{area}^{Ru-CoSe_2}(mA\ cm^{-2})}{mass_{Ru}} = 25.2\ A{\cdot}mg^{-1} \quad (8)$$

$$j_{mass}^{PtC} = \frac{j_{area}^{PtC}(mA\ cm^{-2})}{mass_{Pt}} = 3.06\ A{\cdot}mg^{-1} \quad (9)$$

**Synthesis of Co-MOF precursor**

Co-MOF was prepared via a co-precipitation method. In a typical synthesis, Solutions A and B were prepared by dissolving $Co(NO_3)_2 \cdot 6H_2O$ (0.6 g) and 2-methylimidazole (1.3 g) in deionized water (30 mL), respectively. Subsequently, Solution A was added into Solution B and the mixture was kept stirring at room temperature for 20 h. The purple color precipitate was then centrifuged, washed 3 times with deionized water, and finally dried under vacuum at 60 °C.

**Synthesis of Ru-$CoSe_2$**

To synthesize Ru-$CoSe_2$, 100 mg as-prepared Co-MOF was dispersed in 30 mL deionized water by sonication for 20 min, and then a given amount of $RuCl_3$ aqueous solution (10 $mg \cdot mL^{-1}$) was added to the resulting suspension. After stirring at 60 °C for 2 h, the black sediment was collected by centrifugation, washed 3 times with deionized water, and then dried under vacuum at 60 °C overnight. Subsequently, the obtained black substance (namely RuCo-MOF) was mixed with selenium powder in a 1:2 mass ratio and subjected to grinding, and then heated in an $N_2$ atmosphere to a designated temperature (300, 400, 500, 600, or 700 °C) at a ramp rate of 5 $°C \cdot min^{-1}$ and held at that temperature for 2 h.

**Synthesis of $CoSe_2$**

The synthesis of $CoSe_2$ was similar to that of Ru-$CoSe_2$ except that $RuCl_3$ was not added. 100 mg of prepared Co-MOF was dispersed by sonication in 30 ml of deionized water for 20 min, followed by stirring at 60 °C for 2 h. The dried product was then mixed with selenium powder

in a 1:2 mass ratio and ground, then heated to 400 °C in a nitrogen atmosphere at an elevated rate of 5 °C-min$^{-1}$ and held at this temperature for 2 hours.

**Synthesis of $V_{Se}$-$CoSe_2$**

To synthesize $V_{Se}$-$CoSe_2$, the as-prepared $CoSe_2$ was heated in a tube furnace to 400 °C at a ramp rate of 2 °C·min$^{-1}$ and then held for 2 h under $N_2/H_2$ atmosphere (95/5 %).

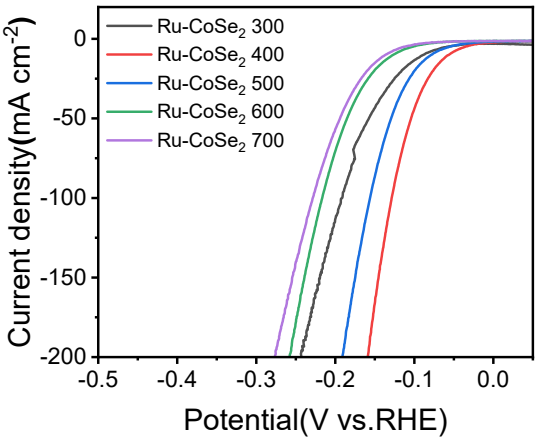


**Figure S1**. Polarization curves of Ru-$CoSe_2$ prepared by different selenization temperatures of 300, 400, 500, 600 and 700 ℃ in alkaline solution.

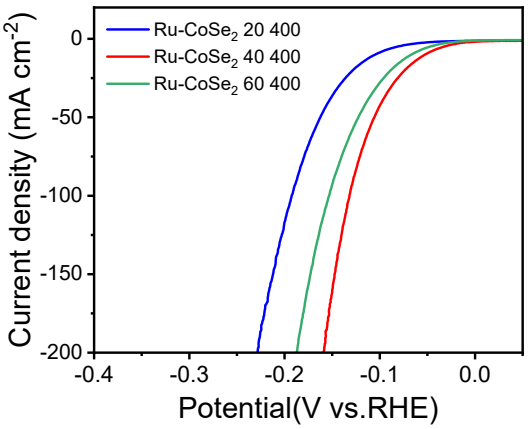


**Figure S2**. Polarization curves of Ru-$CoSe_2$ prepared in alkaline solution with different $RuCl_3$ doping levels of 20 mg, 40 mg, and 60 mg. The Ru-$CoSe_2$ prepared with $RuCl_3$ mass of 40 mg shows the highest HER performance.

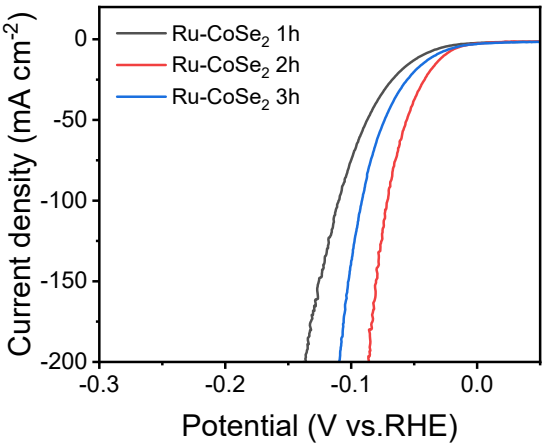


**Figure S3**. Polarization curves of Ru-$CoSe_2$ prepared in alkaline solution at 400 °C for different holding times of 1h, 2 h, and 3h, Ru-$V_{Se}$-$CoSe_2$ prepared by the hydrogenation process at a holding time of 2 h exhibits the highest HER performance.

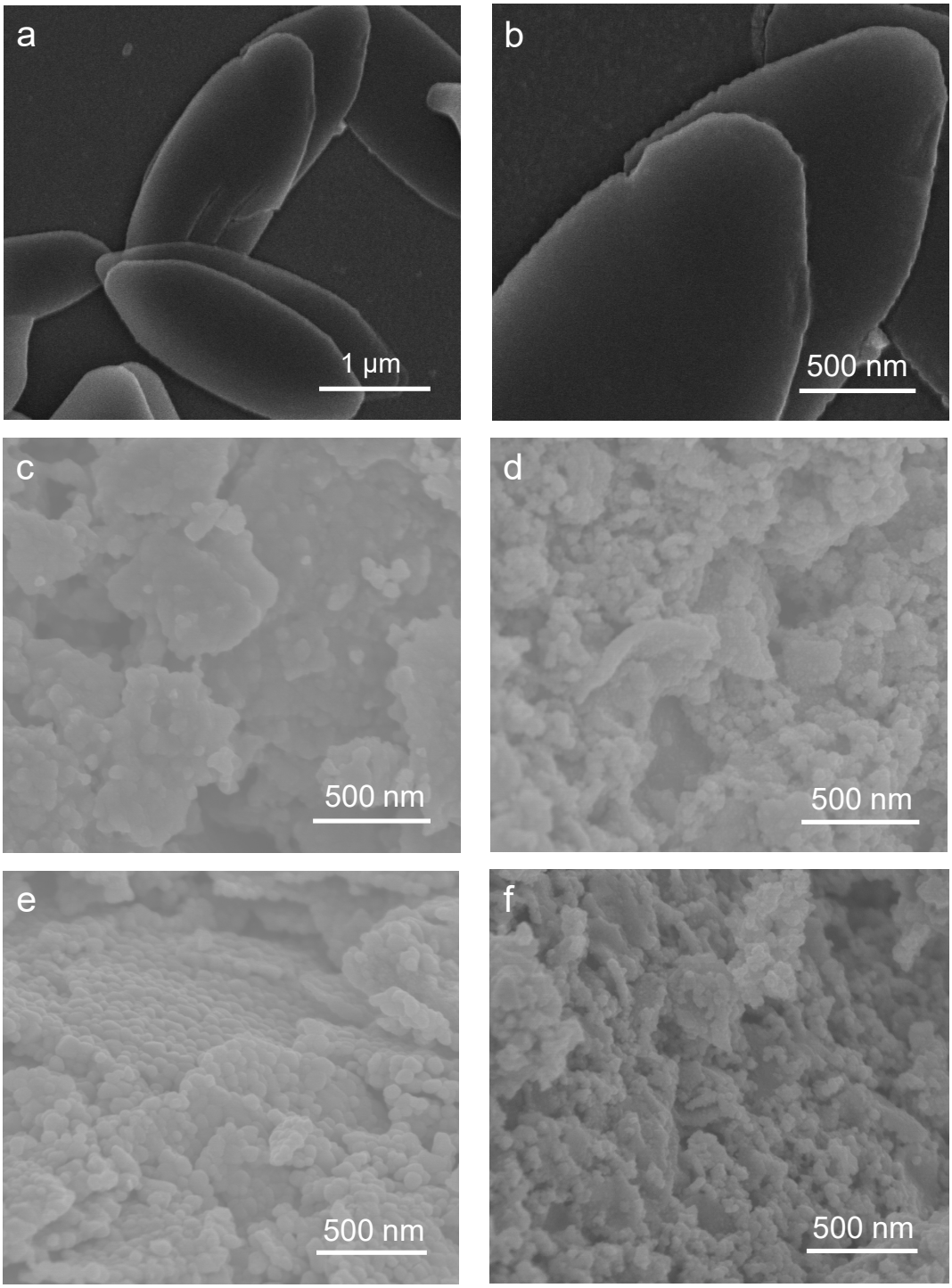


**Figure S4**. SEM images of Co-MOF (a,b), $CoSe_2$ (c), Ru-$CoSe_2$ (d), $V_{Se}$-$CoSe_2$ (e), and Ru-$V_{Se}$-$CoSe_2$ (f).

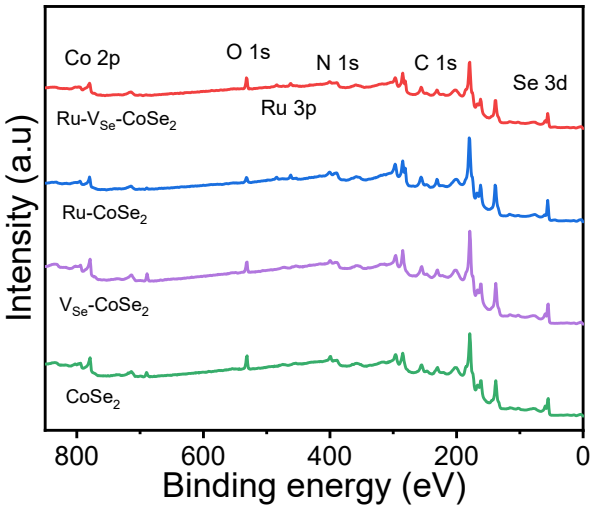


**Figure S5.** XPS survey spectra of Ru-$V_{Se}$-$CoSe_2$, Ru-$CoSe_2$, $V_{Se}$-$CoSe_2$, and $CoSe_2$.

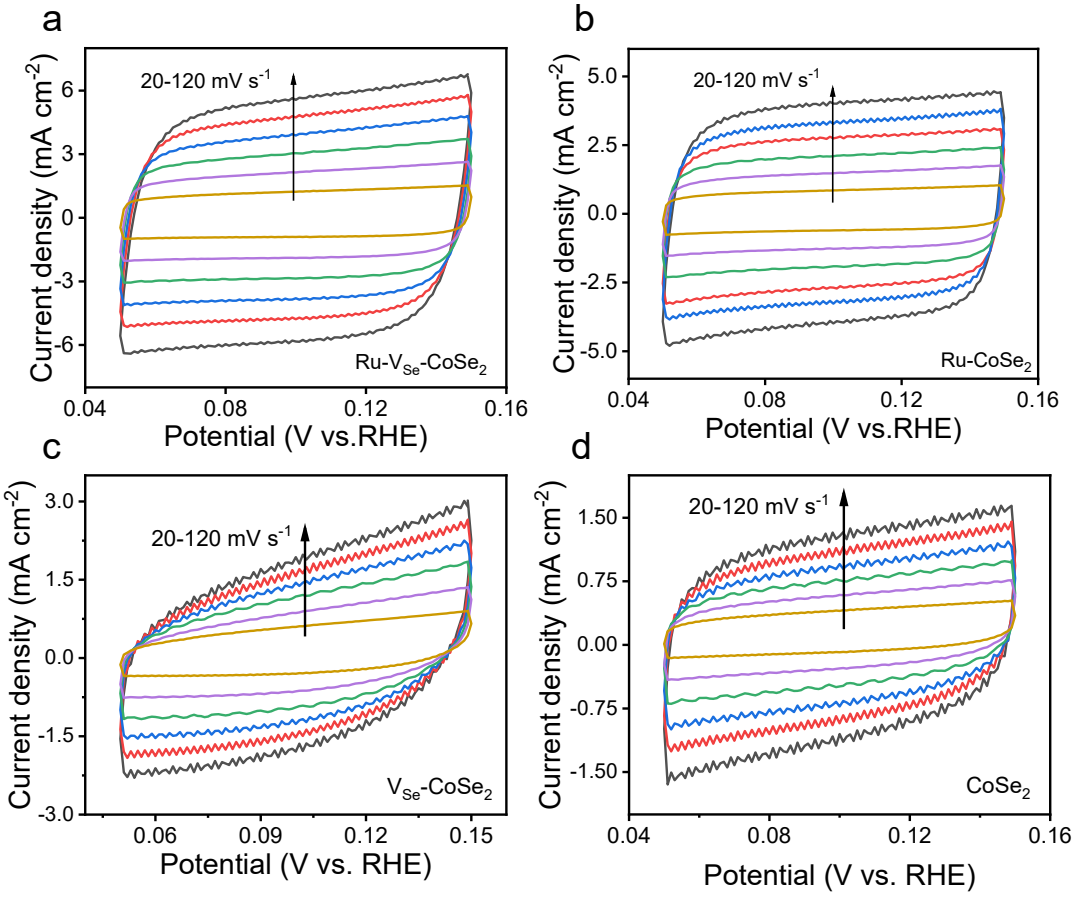


**Figure S6.** Electrochemical double-layer capacitance measurements of Ru-$V_{Se}$-$CoSe_2$ (a), Ru-$CoSe_2$ (b), $V_{Se}$-$CoSe_2$ (c), and $CoSe_2$ (d).

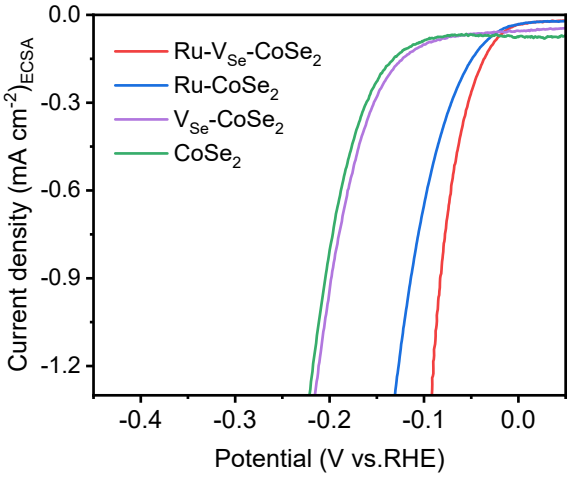


**Fig. S7**. ECSA normalized polarization curves of Ru-$V_{Se}$-$CoSe_2$, Ru-$CoSe_2$, $V_{Se}$-$CoSe_2$, and $CoSe_2$.

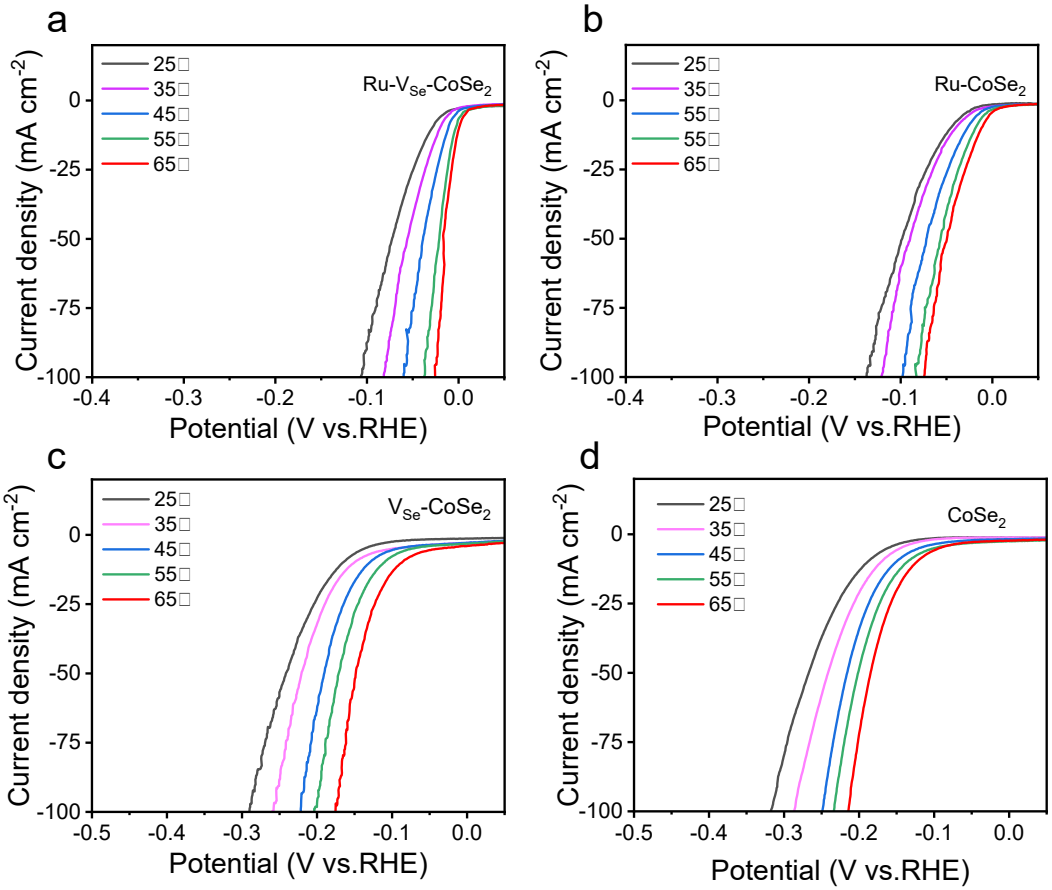


**Figure S8.** Polarization curves of Ru-$V_{Se}$-$CoSe_2$ (a), Ru-$CoSe_2$ (b), $V_{Se}$-$CoSe_2$ (c), and $CoSe_2$ (d) at different temperatures.

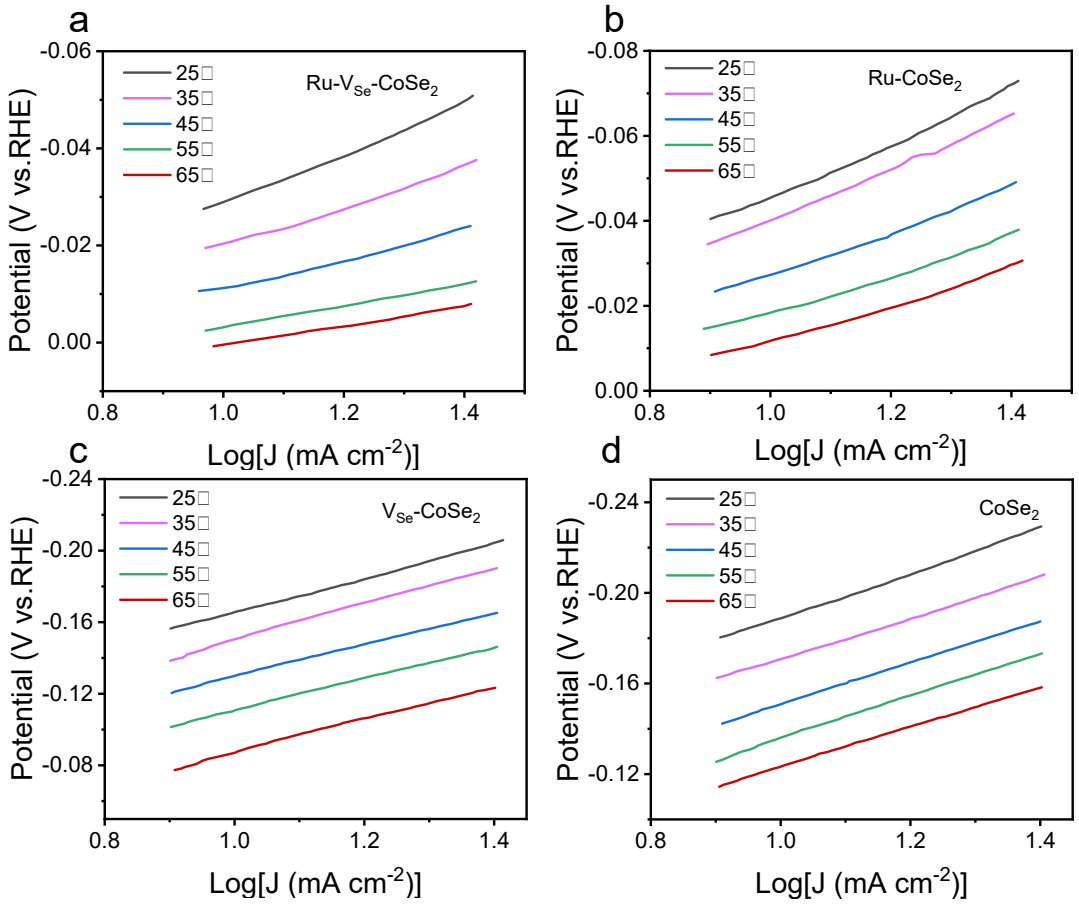


**Figure S9.** Tafel slopes of Ru-$V_{Se}$-$CoSe_2$ (a), Ru-$CoSe_2$ (b), $V_{Se}$-$CoSe_2$ (c), and $CoSe_2$ (d) at different temperatures.

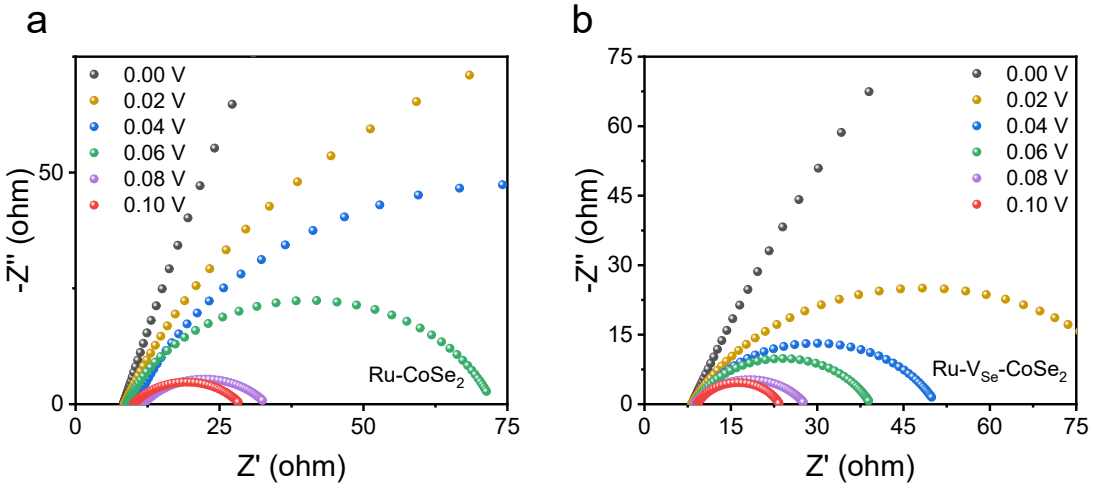


**Figure S10**. Nyquist plots for Ru-$CoSe_2$ (a) and Ru-$V_{Se}$-$CoSe_2$ (b) at different applied potentials in 1.0 M KOH

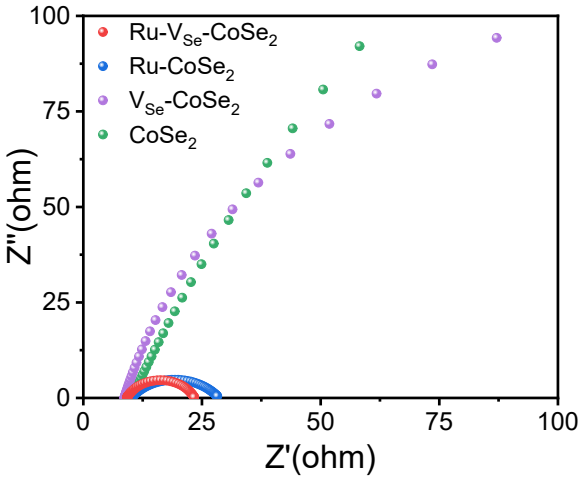


**Figure S11.** Nyquist plots of Ru-$V_{Se}$-$CoSe_2$, Ru-$CoSe_2$, $V_{Se}$-$CoSe_2$ and $CoSe_2$ at 0.1 V (vs. RHE).

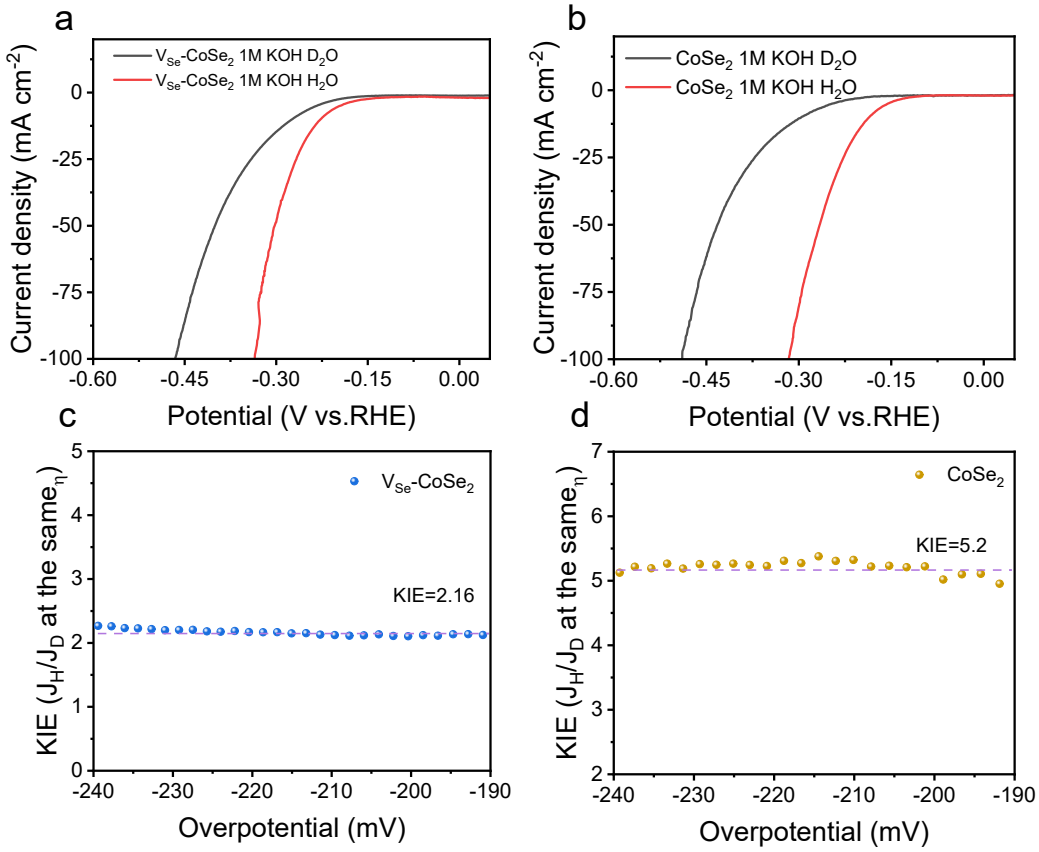


**Figure S12** Polarization curves of $V_{Se}$-$CoSe_2$ (a) and $CoSe_2$ (b) in 1.0 M KOH $H_2O$ solution and 1.0 M KOH $D_2O$ solution and the KIE values vs. overpotential of $V_{Se}$-$CoSe_2$ (c) and $CoSe_2$ (d).

**Table S1.** The corresponding elemental compositions of Ru-$V_{Se}$-$CoSe_2$, and Ru-$CoSe_2$ obtained from ICP results.

| Sample | Ru wt.% | Co wt.% |
|---|---|---|
| Ru-$V_{Se}$-$CoSe_2$ | 2.44 | 17.34 |
| Ru-$CoSe_2$ | 2.40 | 16.63 |

**Table S2:** The EIS fitting results of Ru-$V_{Se}$-$CoSe_2$, Ru-$CoSe_2$, $V_{Se}$-$CoSe_2$ and $CoSe_2$

| Sample | $R_s$ /Ω | $R_{ct}$ /Ω |
|---|---|---|
| Ru-$V_{Se}$-$CoSe_2$ | 9.2 | 14.3 |
| Ru-$CoSe_2$ | 10.1 | 18.5 |
| $V_{Se}$-$CoSe_2$ | 8.7 | 288.5 |
| $CoSe_2$ | 10.3 | 739.3 |

**Table S3**. Comparison of HER performance of Ru-$V_{Se}$-$CoSe_2$ with other reported Ru-doped HER catalysts in alkaline solution.

| Reference | Catalyst | Current density (J) | Potential at the corresponding J (mV) | Electrolyte |
|---|---|---|---|---|
| **This work** | **Ru-$V_{Se}$-$CoSe_2$** | **10 mA·cm$^{-2}$** | **29** | **1.0 M KOH** |
| *Small Methods* **2023,** *7* (2), 2201362 | α-$Co(OH)_2$@Ru | 10 mA·cm$^{-2}$ | 30 | 1.0 M KOH |
| *Nano Energy* **2021,** *85*, 105940 | Ru/$Co_3O_4$ | 10 mA·cm$^{-2}$ | 31 | 1.0 M KOH |
| *Appl Catal B-Environ* **2021,** *298*. 120557 | Ru/Ni-$MoS_2$ | 10 mA·cm$^{-2}$ | 32 | 1.0 M KOH |
| *Chem Eng J* **2022,** *433,* 133517 | Ru/$Co(OH)_2$ | 10 mA·cm$^{-2}$ | 35 | 1.0 M KOH |
| *Adv Energy Mater* **2023,** *13* (20), 2204177 | RuCo-CAT /CC | 10 mA·cm$^{-2}$ | 38 | 1.0 M KOH |
| *Appl Catal B-Environ* **2020,** *277*. 119236 | Ru SAs / N-$Mo_2C$ NSs | 10 mA·cm$^{-2}$ | 43 | 1.0 M KOH |
| *Applied Catalysis B-Environmental* **2020,** *263*. 118324 | Ru-NiFe-P | 10 mA·cm$^{-2}$ | 44 | 1.0 M KOH |
| *Angew Chem Int Edit* **2020,** *59* (39), 17219-17224. | (Ru-Co)$O_x$ | 10 mA·cm$^{-2}$ | 44 | 1.0 M KOH |
| *Appl Catal B-Environ* **2023,** *324*, 122294 | $RuO_2$@$Co_3O_4$(1:6) | 10 mA·cm$^{-2}$ | 45 | 1.0 M KOH |
| *J Energy Chem* **2023,** *87*, 286-294. | Co-Ru/NCN | 10 mA·cm$^{-2}$ | 62 | 1.0 M KOH |
| *Small Methods* **2019,** *3* (12) 1900653 | SA-Ru-MoS | 10 mA·cm$^{-2}$ | 76 | 1.0 M KOH |
| *Chem Eng J* **2023**, 451, 138977 | 3D $Mo_2C$ (1:1) | 10 mA·cm$^{-2}$ | 110 | 1.0 M KOH |